RSCPublishing   Faraday Discussions

FD175:Prolonging the Circulatory Retention of SPIONs Using Dextran Sulfate: In Vivo Tracking Achieved by Fuctionalisation with Near Infrared Dyes

Journal:	*Faraday Discussions*
Manuscript ID:	FD-ART-05-2014-000114
Article Type:	Paper
Date Submitted by the Author:	20-May-2014
Complete List of Authors:	Abdollah, Maha; UCL, Cancer Institute Kalber, Tammy; UCL, Centre for Advanced Biomedical Imaging Tolner, Berend; UCL, Cancer Institute Southern, Paul; The Royal Institution of Great Britain, UCL Healthcare and Biomagnetics Laboratory Bear, Joseph; University College London, Department of Chemistry Robson, Mathew; UCL, Cancer Institute Pedley, Barbara; UCL, Cancer Institute Parkin, Ivan; University College London, Department of Chemistry Pankhurst, Quentin; University College London, Department of Physics + Astronomy Mulholland, Paul; UCL, Cancer Institute Chester, Kerry; UCL, Cancer Institute

SCHOLARONE™
Manuscripts

Prolonging the Circulatory Retention of SPIONs Using Dextran Sulfate: In Vivo Tracking Achieved by Fuctionalisation with Near Infrared Dyes

5 **Maha R.A. Abdollah[a],* Tammy Kalber[b], Berend Tolner[a], Paul Southern[c], Joseph C. Bear[d], Mathew Robson[a], R. Barbara Pedley[a], Ivan P. Parkin[d], Quentin Pankhurst[c], Paul Mulholland[a] and Kerry Chester[a]**

DOI: 10.1039/b000000x [DO NOT ALTER/DELETE THIS TEXT]

10 The rapid reticuloendothelial system (RES) mediated clearance of superparamagnetic iron oxide nanoparticles (SPIONs) from circulation is considered a major limitation of their clinical utility. We aimed to address this by using dextran sulfate 500 (DSO4 500), a Kupffer cell blocking agent, to prolong SPIONs circulatory time. Blood concentrations of 15 SPIONs are difficult to quantify due to the presence of haemoglobin. Therefore we developed methods to functionalize SPIONs with near infrared (NIR) dyes in order to trace their biodistribution. Two SPIONs were investigated: Nanomag-D-spio-NH$_2$ and Ferucarbotran. Nanomag-D-spio-NH$_2$ was functionalised using NHS ester NIR dye and Ferucarbotran 20 was labelled using periodate oxidation followed by reductive amination or a combination of EDC/NHS and click chemistries. Stability after conjugation was confirmed by dynamic light scattering (DLS), superconducting quantum interference device (SQUID) and transmission electron microscopy (TEM). *In vivo* experiments with the functionalised SPIONs 25 showed a significant improvement in SPIONs blood concentrations in mice pre-treated with DSO4 500.

Introduction

Superparamagnetic iron oxide nanoparticles (SPIONs) provide a versatile platform for biomedical applications[1] due to their inducible magnetic properties 30 (superparamagnetism) [2]. Potential applications include magnetic resonance imaging (MRI) [3-7], hyperthermia [8-11], drug delivery [12-14], stem cell labelling and tracking [15-17], tissue repair and cell separation [12]. To date the most established clinical use of SPIONs is for MRI contrast enhancement to detect focal liver and spleen cancerous lesions with SPIONs such as Endorem® (Ferridex® in US) and Resovist® 35 (Ferucarbotran) [6, 18].

[a] UCL Cancer Institute, University College London (UCL), Paul O'Gorman Building, 72 Huntley Street, London, WC1E 6BT, UK. Tel: +44 20 7679 0700; E-mail: k.chester@ucl.ac.uk
[b] Centre for Advanced Biomedical Imaging, UCL, London, UK.
[c] UCL Healthcare and Biomagnetics Laboratory, The Royal Institution of Great Britain, London, UK.
[d] Department of Chemistry, UCL, London, UK.

When administered intravenously, SPIONs are rapidly cleared from the circulation by the reticuloendothelial system (RES) [19], with uptake dependent on factors such as the hydrodynamic diameter, electrical charge and surface coating [20]. Thus, in patients, approximately 80% of the injected dose of Ferucarbotran rapidly accumulates in the liver within minutes resulting in a distribution half-life of only 3.9 to 5.8 minutes and an elimination half-life of 2.4-3.6 hours [6]. The preferential uptake of SPIONs by the liver and spleen RES is the property exploited for MRI because it reveals liver tumour deposits as negative images [6]. However, the rapid clearance of the SPIONs from the circulation is considered as one of the main challenges for applications other than those dependent on RES targeting. We hypothesized that the uptake of SPIONs by macrophages could be blocked by dextran sulphate sodium salt 500 (DSO4 500), enabling further development of SPIONs and expanding their clinical potential for exciting new applications such as magnetic hyperthermia in cancer [9, 11].

We aimed to investigate the possibility of using DSO4 500 to block uptake of Ferucarbotran by RES *in vivo* and thus increase its blood residence time. This would necessitate tracing the blood concentrations of SPIONs, which can be difficult because haemoglobin interferes with iron quantification assays. Alternative methods such as incorporation of radioactive iron isotopes (e.g. ^{59}Fe) during the synthesis process of SPIONs [21] require bespoke manufacture. Other approaches utilise the ability of SPIONs to shorten the proton relaxation time of water by MR [3] or magnetic susceptibility measurements (MSM) via a magneto-susceptometer [22].

We designed a new method to trace blood concentrations of SPIONs by labelling them with near infrared (NIR) dyes. NIR labelling has been used extensively for non-invasive *in vivo* imaging [23]. The molar extinction coefficients of haemoglobin and oxyhaemoglobin are at their lowest in the NIR range, especially around wavelengths of 800 nm [24], which is predicted to give the least background if NIR-dye labelled SPIONs were to be measured in whole blood.

Two dextran coated SPIONs were investigated: Ferucarbotran and Nanomag®-D-spio amine. Nanomag®-D-spio amine are dextran coated amine functionalised nanoparticles with hydrodynamic diameter in the range of 50-120 nm [25]. The presence of amine (NH_2) groups on the SPIONs surface is ideal for conjugation to NHS ester dyes, therefore Nanomag®-D-spio amine was first investigated as a proof-of-concept. However, our main SPION of interest is Ferucarbotran, the active ingredient of Resovist® (SHU 555A) a clinical MRI contrast agent [6] previously marketed by Schering AG, Berlin, Germany and currently produced by Fujifilm RI Pharma Co., Tokyo, Japan. Resovist® has an average hydrodynamic diameter of 60 nm and consists of a mixture of magnetite-Fe_3O_4 and maghemite-γFe_2O_3 crystals embedded in a biocompatible carboxydextran shell that provides stability of the particles both in solution and *in vivo* [2, 6]. The well documented safety profile of Ferucarbotran in pre-clinical studies [4] and in patients [3, 6, 26-29] make it an attractive agent for development for therapeutic use. In particular, when placed in an alternating magnetic field, Ferucarbotran can be induced to heat by a process known as magnetic field hyperthermia. Temperatures as high as 72.4 ^{0}C *in vitro* and 45 ^{0}C-59.9 ^{0}C *in vivo* have been achieved [30-34], indicating that Ferucarbotran has potential for localised hyperthermic cancer treatment. The conjugation of carboxydextran coated Ferucarbotran has proved to be challenging and thus a combination of EDC/NHS and click chemistry was devised in order to functionalise Ferucarbotran

with a NIR dye.

Materials and Methods

All chemicals were purchased from Sigma Aldrich unless otherwise specified.

Superparamagnetic iron oxide nanoparticles (SPIONs)

5 Details of the SPIONs investigated as stated by the manufacturers are shown in Table 1 and a schematic presentation of a SPION is shown in Figure 1.

Table 1: List of nanoparticles investigated.

SPION	Supplier	Size range	Coating	Functional groups	Iron concentration
Ferucarbotran (FC)	Meito Sangyo Co. LTD., Japan	45-65 nm	Carboxydextran	OH, COOH (Hydroxyl and carboxylic)	55.6 mg/ml
Nanomag®-D-spio-amine (NM)	Micromod Partikeltechnologie GmbH, Germany	50-120 nm	Dextran	NH$_2$ (amine)	2.4 mg/ml
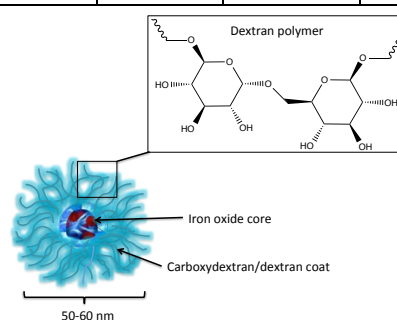
Figure 1: Schematic presentation of a SPION illustrating the iron oxide core embedded in dextran (Nanomag-D-spio-amine) or carboxydextran (Ferucarbotran) coating. Inset: the chemical structure 10 of dextran polymer, which is made up of repeated glucose unites.

Characterisation of SPIONs

Dynamic Light Scattering (DLS)

SPIONs were characterised before and after functionalisation using a Zetasizer Nano ZS90 (Malvern, Worcestershire, UK) to identify their hydrodynamic diameter and 15 zeta potential. SPIONs solutions were prepared in sterile-filtered 5 mM NaCl.

Transmission Electron Microscopy (TEM)

SPIONs samples were diluted in distilled water and visualised with a Jeol 2100 HRTEM with a LaB$_6$ source operating at an acceleration voltage of 200 kV with an Oxford Instrument UTW EDX detector running AZTEC software. Micrographs were taken in a 20 Gatan-Orius charge coupled device (CCD). Core sizes were measured from TEM images using ImageJ software.

Superconducting Quantum Interference Device (SQUID)

Samples were prepared for SQUID magnetometry by pipetting 5 µl of solution into a

polycarbonate powder capsule filled with cotton wool to absorb the liquid. The sample was then left to dry for 2 hours before mounting onto a brass SQUID-VSM rod. A Quantum Design MPMS SQUID VSM Evercool system (Quantum Design, San Diego, USA) was used to measure the magnetic moment as a function of field
5 between ±7T at 300K at atmospheric pressure.

Near infrared (NIR) dyes

Three near infrared dyes were used to functionalise the SPIONs (Table 2).

Table 2: List of near infrared (NIR) dyes used.

Product	Supplier	Functional group	Reactivity
DyLight® 800 NHS ester	Thermo Scientific, Pierce Biotechnology	NHS ester (N-Hydroxysuccinimide)	Amine
iFluor™ 780 amine	Stratech Scientific Ltd.	Amine	Carbonyl (aldehydes)
IRDye® 800 CW azide	LI-COR Biosciences	Azide	Copper free click reaction with dibenzocyclooctyne (DBCO)

RES blockers

10 DSO4 500 was used as an RES blocker in doses ranging from 3 to 30 mg/kg. DSO4 500 has an average molecular weight of >500,000 Daltons (Sigma Aldrich data sheet, product code: D6001)

Conjugation of Nanomag®-D-spio-NH$_2$ to DyLight® 800 NHS ester dye (Figure 2)

The particles were purchased as a suspension in water, which is incompatible with
15 the labelling protocol. Consequently, water was exchanged with 50 mM sodium borate buffer (pH 8.5) using a PD-10 desalting column (GE Healthcare, UK).

500 µl of 50 mM sodium borate buffer was added to 50 µg of the lyophilized dye. The resultant dye solution was subsequently added to 1 ml of SPIONs (2.4 mg Fe) solution. The reaction was allowed to proceed for 1 hour at room temperature (RT)
20 on a roto-torque. The solution was purified by applying the sample to a PD-10 column equilibrated with PBS.
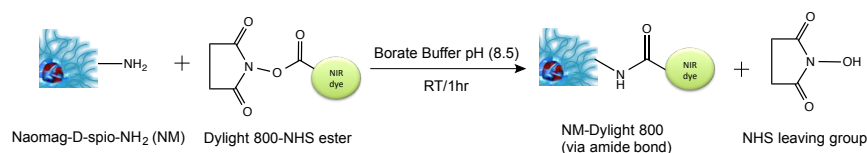

Figure 2: Schematic presentation of the chemical reaction between Nanomag®-D-spio-NH$_2$ (NM) and DyLight® 800 NHS ester dye. The NHS ester attacks the amine groups on the surface of the SPIONs to form a stable amide bond. The reaction was allowed to proceed for 1 hour at RT.

25

Conjugation of Ferucarbotran to DyLight® 800 NHS ester using epichlorohydrin (Figure 3)

The protocol was derived from the procedures described by Pittet *et al.* 2006 [35] and Maxwell *et al.* 2007 [36]. In a conical flask, 200 μl of Ferucarbotran (11 mg Fe) was diluted into 800 μl of distilled water. Then 1.6 ml of 5 M sodium hydroxide (NaOH) was added and the solution was allowed to react for 15 minutes at RT with vigorous agitation on a shaking platform before 0.7 ml of epichlorohydrin solution was added and the solution was left to react on the shaking platform at RT for 8 hours. Next 0.6 ml of 25% v/v of ammonia solution was added and the solution was left at RT for 10 hours while shaking. Finally the solution was extensively dialysed against distilled water to remove excess epichlorohydrin using a dialysis cassette with 20 K cut off (Thermo Fisher Scientific). The aminated Ferucarbotran was subsequently labelled with DyLight® 800 NHS ester using the protocol described above for Nanomag-D-spio-NH_2.
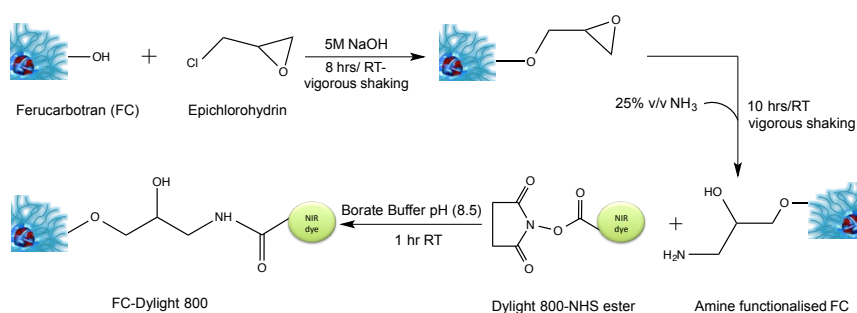

Figure 3: Schematic presentation of the amination of Ferucarbotran (FC) using epichlorohydrin followed by reaction with DyLight® 800 NHS ester NIR dye.

Conjugation of Ferucarbotran to iFluor™ 780 amine using periodate oxidation followed by reductive amination (Figure 4)

The protocol was derived from Vigor *et al.* 2012 [37]. Ferucarbotran is suspended in water, which was exchanged with 50 mM sodium borate buffer (pH 8.5) using a PD-10 desalting column. Ferucarbotran (200 μl, 11 mg Fe) was added to a 10 mg/ml solution of sodium periodate ($NaIO_4$) in 50 mM sodium borate buffer (pH 8.5). The reaction was allowed to proceed for 25-30 minutes in the dark on a roto-torque and then terminated by running the sample on a PD-10 column equilibrated with 50 mM borate buffer (pH 8.5). 100 μl of 0.1 mg/ml of iFluor™ 780 amine NIR dye was added to the reaction mixture and left to react for 2 hours at RT on a roto-torque. Finally 10 μl of 5 M sodium cyanoborohydride ($NaCNBH_3$) in 1 M NaOH solution was added per 1 ml of reaction mixture. The reaction was left on roto-torque for 24 hours then purified by passing it twice through a PD-10 column equilibrated with PBS.
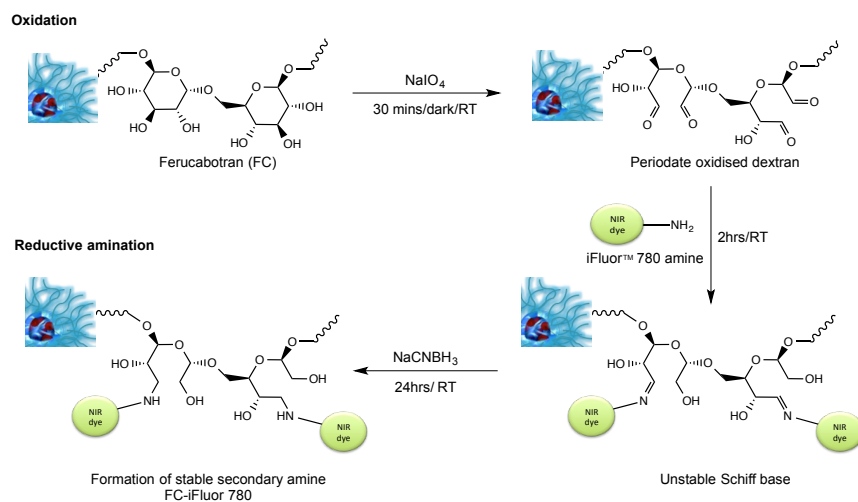
Oxidation

Reductive amination

Figure 4: A schematic presentation of the 2-step reaction to conjugate Ferucarbotran (FC) to iFluor 780 amine. The reaction has two main steps: first the oxidation of the hydroxyl groups on the dextran coat of FC with sodium periodate followed by the reductive amination using NaCNBH$_3$ to
5 form a stable amine conjugate.

Conjugation of Ferucarbotran to IRdye® 800CW azide using EDC/NHS and click chemistries (Figure 5)

Ferucarbotran (88.6 μl, 5 mg Fe) was incubated with 200 μl of EDC/sulfo-NHS (1-Ethyl-3-[3-dimethylaminopropyl]carbodiimide-hydrochloride/(N-
10 hydroxysulfosuccinimide; Thermo Fisher Scientific) activation buffer (1.21 mg EDC and 8.8 μl of 230 mM sulfo-NHS prepared in 0.1 M MES buffer, pH=6). The reaction was allowed to proceed for 20 minutes at room temperature (on a rotator) and was terminated by application to a PD-10 column equilibrated with PBS (pH=7.4). Next, 200 μg of dibenzocyclooctyne-amine (DBCO-NH$_2$) linker in 1 ml
15 PBS was added to the reaction mixture and incubated for 2 hours at RT followed by 100 μl/ml of 25 mM glycine for 30 minutes to block the remaining reactive sites. The sample (FC-NH-DBCO conjugate) was buffer exchanged using a PBS-equilibrated PD-10 column to remove unreacted linker. Finally, 2.5 μl of 20 mg/ml (~50 μg) of IRDye® 800 CW azide was incubated with the FC-NH-DBCO conjugate
20 for 3 hours at 37 ^{0}C in a water bath. The resultant NIR-conjugated SPIONs were extensively purified by passing, at least 3x, through PD-10 columns equilibrated with PBS to remove any dye that was unspecifically attached to the dextran coat of Ferucarbotran.
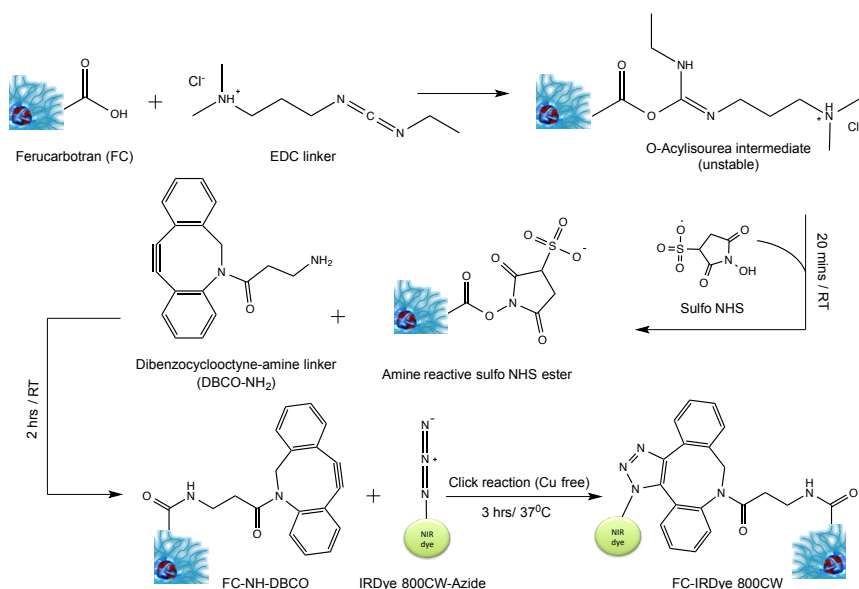
25

Figure 5: Schematic presentation of the labelling reaction of Ferucarbotran (FC) with IRDye®
800CW-Azide. This method combines the activation of the COOH groups present on the
carboxydextran coat of FC using EDC/NHS to react with a DBCO-amine linker. The conjugate is
then "clicked" with azide functionalised NIR dye (IRDye® 800CW-Azide).

Following all SPIONs conjugations, the integrated signal intensity of a serial
dilution of known iron concentrations of the conjugates was measured at 800 nm on
Odyssey® infrared scanner (LI-COR Biosciences, Lincoln, Nebraska, USA) to plot a
standard curve. Integrated signal intensity (also known as pixel volume) is defined
by the Odyssey® infrared scanner software as the sum of the intensity values for all
pixels enclosed by a shape, multiplied by the area of the shape (counts mm^2).

In vivo blocking of the uptake of SPIONs by the RES

All *in vivo* experiments were performed using mouse models in compliance with
licenses issued under the U.K. Animals (Scientific Procedures) Act 1986 after local
ethical committee review. All mice were 6-8 week old female BALB/c (Charles
River Laboratories, UK). The mice had an average weight of 20 g at the start of the
experiments. All labelled SPIONs were injected at a dose of 10 μmolFe/kg. A
general layout of the experimental design is shown in Figure 6. SPIONs and DSO4
500 were prepared in PBS and sterile filtered (using 0.22 μm syringe filter) in a cell
culture hood prior to injections to minimise bacterial contamination. All injections
were administered intravenously through tail veins.

For Nanomag-D-spio-DyLight 800 (NM-DyLight 800), DSO4 500 was injected at
doses ranging from 3 to 30 mg/kg. A period of 24 hours was given to allow for
sufficient blocking of the liver by DSO4 500 then NM-DyLight 800 was injected.

For Ferucarbotran-iFluor™ 780 (FC-iFluor 780), 30 mg/kg of DSO4 500 was
injected and after 24 hours FC-iFluor 780 was injected.

For Ferucarbotran-IRDye® 800CW (FC-IRDye 800), 30 mg/kg of DSO4 500 was injected. A period of 0, 2 or 24 hours was given before FC-IRDye 800 was administered.

One hour following the injection of the dye labelled SPIONs, the mice were
5 anaesthetized using a 1% isoflurane (Ivax Pharmaceuticals, UK) oxygen mixture. Blood was collected by cardiac puncture in EDTA-coated tubes (Teklab or BD Vacutainer®) and the mice were sacrificed by cervical dislocation. For SPIONs quantification, a 100 µl aliquot of each blood sample was transferred into a 96-well plate (Corning) and then the integrated signal intensity was measured at 800 nm on
10 an Odyssey® infrared scanner.
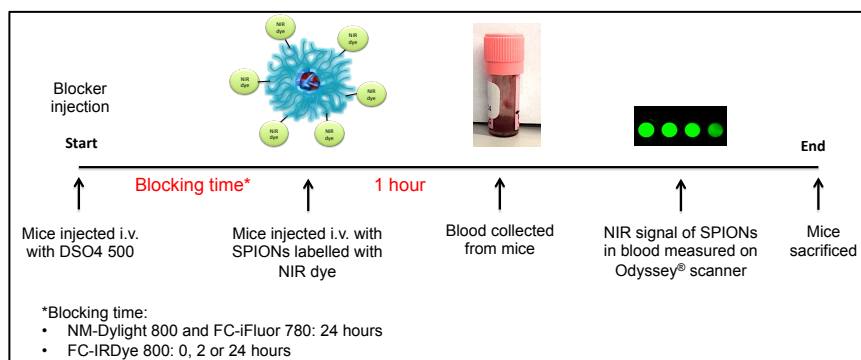
Figure 6: Experimental design of the *in vivo* blocking experiments. DSO4 500 was injected intravenously then a certain blocking period was allowed ranging from 0 to 24 hours depending on the SPIONs investigated. After which NIR dye labelled SPIONs (either NM-DyLight 800, FC-iFluor 780 or FC-IRDye 800) were injected intravenously. 1 hour following SPIONs injection blood
15 was collected from mice and measured on Odyssey® scanner.

Statistical analysis

For NM-DyLight 800 and FC-IRDye 800 *in vivo* experiments, the effect of blocking was assessed using a total of 8 mice per group in 4 independent experiments (2-mice/group for NM-DyLight 800 and 1-3 mice/group for FC-IRDye 800). An
20 ANOVA test was used to assess variance associated with the different experiments, and statistical significance between groups (blocked versus unblocked) was assessed using a Tukey HSD test on the fitted model. For FC-IRDye 800 final experiment (Figure 17) Shapiro-Wilk test confirmed that the data was normally distributed, and therefore a Student's unpaired 2-tailed t-test was used to assess statistical
25 significance of the data. p values less than 0.05 were considered statistically significant.

Results

Characterisation of SPIONs

Unmodified and dye conjugated SPIONs were characterised on DLS to monitor
30 changes in their overall size and charge due to functionalisation. In general, only minor differences were observed between functionalised and unmodified SPIONs (Table 3). The exception, FC-iFluor 780, showed a 26.1 nm increase in diameter, an

increase in the Zeta potential by -14.5 mV, and an increase in polydispersity index (PDI) to 0.36. Precipitations in SPIONs solution were observed by visual inspection following the reaction. These changes may be an indication of destabilisation caused by the conjugation reaction.

5 **Table 3:** Characterisation data of SPIONs

Sample	Hydrodynamic diameter		Zeta Potential (mV)	
	Z-Average (nm)	PDI	Mean (mV)	Zeta Deviation (mV)
FC Batch A*	59	0.22	-28.1	3.41
FC-IRDye 800	64.8	0.24	-33.7	13.9
FC Batch B*	56.7	0.20	-29.4	4.02
FC-iFluor 780	82.8	0.36	-43.9	5.56
NM	75.4	0.19	-4.21	9.69
NM-Dyight 800	74.3	0.21	-3.82	7

*2 different batches of Ferucarbotran (FC) were used. Batch A was used in FC-IRDye 800 and batch B in FC-iFluor 780. NM=Nanomag-D-spio-NH_2 (unmodified)

High resolution (HR) TEM was used to investigate the SPIONs iron oxide cores. All
10 samples of Ferucarbotran and Nanomag-D-spio-NH_2 appeared highly crystalline in this assessment and the iron oxide cores appeared to be unaffected by the conjugation process. Average cores sizes were 3.75 ($\pm$ 0.83) nm for Ferucarbotran and 6.02 ($\pm$ 1.82) nm for Nanomag-D-spio-NH_2 (Figure 7 and 8).

SQUID magnetometry was used to test the effect of conjugation on the
15 superparamagnetic properties of both SPIONs. The normalised magnetisation versus field curves show little or no difference between the unmodified SPIONs solution and the conjugated samples, all showing hysteretic behaviour indicating that the magnetic particles are superparamagnetic at 300K (Figure 9).
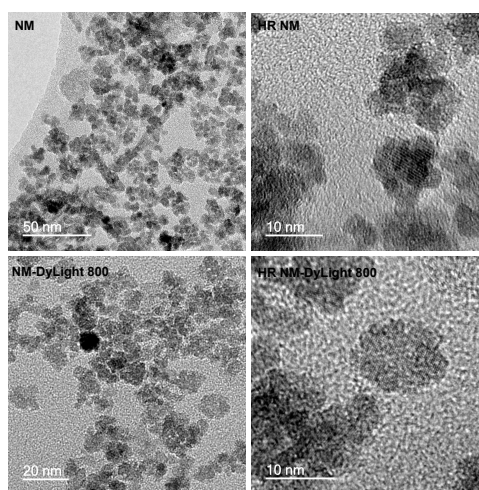
Figure 7: TEM images of Nanomag-D-spio-NH_2 (NM) before and after conjugation to NIR dye.
20 NM appears unaffected by conjugation and HR images (right) are showing lattice planes of iron oxide cores of 6.019 ($\pm$ 1.82) nm in diameter.
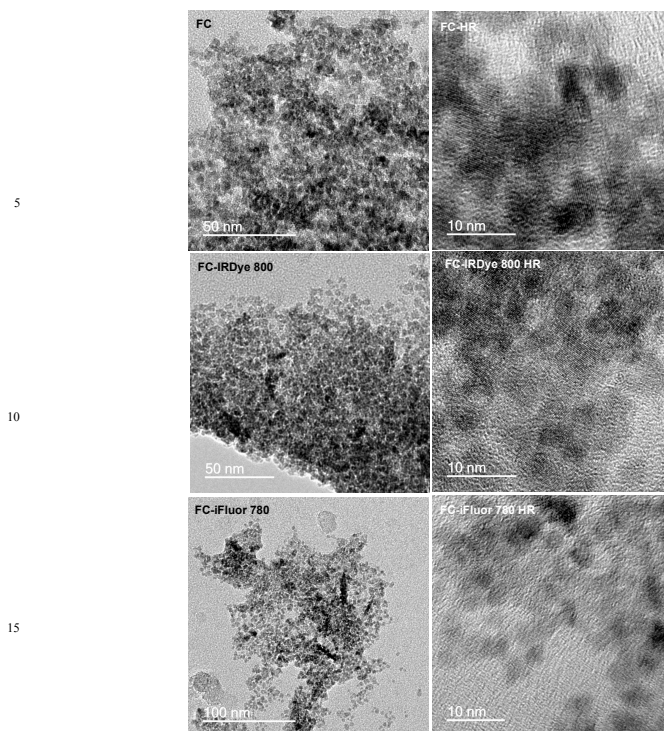
Figure 8: TEM images of Ferucarbotran (FC) before and after conjugation. TEM images have revealed no changes in the iron oxide cores following conjugation. HRTEM images (right) of FC
show iron oxide lattice plains with core sizes of 3.75 (±0.834) nm in diameter.
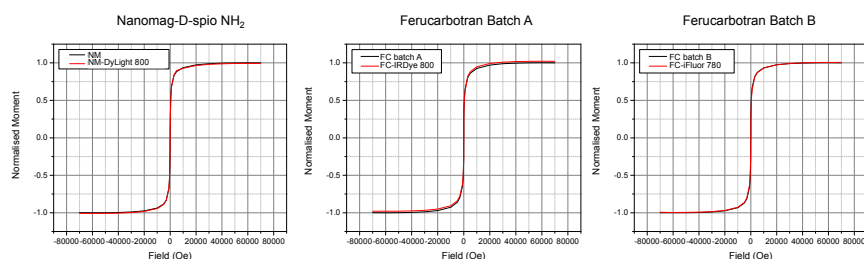

Figure 9: Magnetic hysteresis loops of SPIONs as measured by SQUID magnetometry showing the normalised magnetisation versus field curves. No difference was observed in all the samples measured.

Conjugation of Nanomag-D-spio-amine to NIR dye

Nanomag-D-spio-NH$_2$ SPIONs were used as a proof-of-concept as they could be readily functionalised with a near infrared dye (DyLight® 800 NHS ester) via available amines on the SPION coating. Following the conjugation the samples were measured on Odyssey® scanner and a linear increase in the signal intensity was observed as the iron concentration increased (Figure 10).
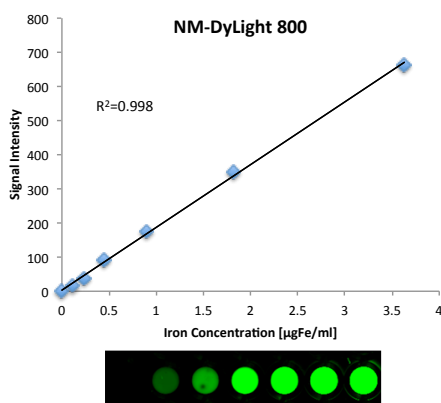
Figure 10: A linear increase (R^2=0.998) in the signal intensity of dye labelled Nanomag-D-spio-NH$_2$ (NM-DyLight 800) was observed as the iron concentration increased. Images of individual wells illustrating florescence intensity are shown below.

The NIR-functionalised SPIONs were used in a pilot experiment (2-mice per group) examining the effects of pre-treatment with DSO4 500 prior to administration of SPIONs. Four DSO4 500 doses were tested: 3, 7.5, 15 and 30 mg/kg. Results showed that the NIR signal intensity of the NIR-labelled SPIONs was strongly enhanced in a dose dependent effect (Figure 11). The highest dose of the blocker (30 mg/kg) was further investigated in four independent 2-mice experiments with different batches of the conjugate. A significant difference was observed (p=0.0016, Tukey HSD test) in the mice pretreated with the blocker DSO4 500 compared to unblocked control. There was a 15.6 times improvement in the median signal intensity of blocked mice compared to unblocked group. (Figure 12)
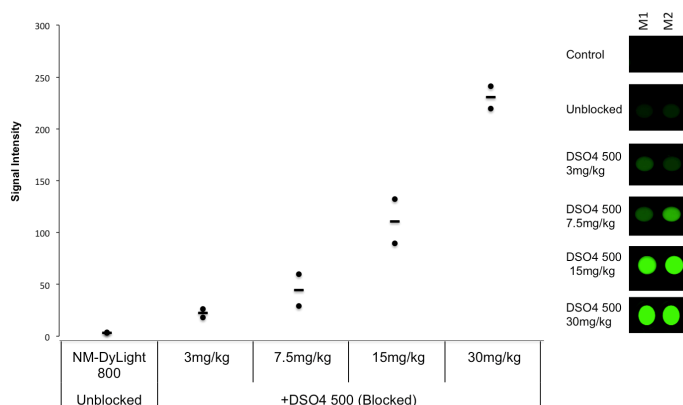

Figure 11: Dot plot showing the mean signal intensity (bar) (n=2) for mice treated with NM-DyLight 800 with and without pre-treatment with different doses of DSO4 500. A dose-dependent increase in the signal intensity was observed as the dose of DSO4 500 increased. Each mouse is represented by a circle (•). Right: Images of individual wells illustrating florescence intensity are shown. M1= mouse 1, M2=mouse 2.
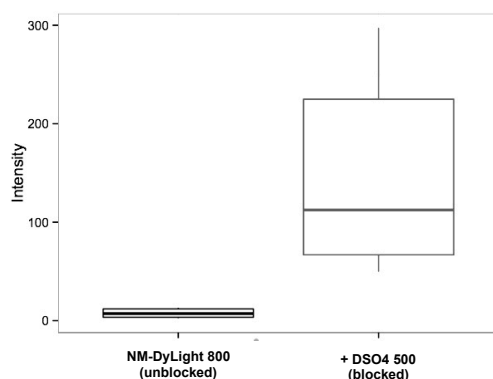
Figure 12: Box plot of all NM-DyLight 800 experiments showing a statistically significant difference between the signal intensity of NM-DyLight 800 in mice pre-treated with the blocker compared to unblocked control. Median signal intensity of blocked group was 112 compared to 7.17 for unblocked mice (p=0.0016).

Conjugation of Ferucarbotran to NIR dyes

Ferucarbotran is coated with carboxydextran and therefore functionalisation is possible to either hydroxyl or carboxylic groups. Nevertheless, labelling Ferucarbotran has proved to be very challenging, due to the destabilising effects of chemical modification, leading to visibly detectable aggregation and precipitation of nanoparticles (Figure 13, B and C).
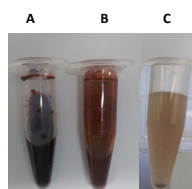

Figure 13: Visual appearance of 3 different Ferucarbotran (FC) solutions. Unmodified FC (A) is a dark brown translucent solution while chemically modified FC, if unstable, can appear as either cloudy (B) or precipitate entirely (C).

We investigated 3 different labelling strategies for Ferucarbotran functionalisation. First amination of the hydroxyl groups using epichlorohydrin was employed [35, 36]. This method, which uses harsh alkali conditions, led to rapid SPIONs destabilisation, with the solution appearing cloudy immediately after the completion of the reaction. The second method combined periodate oxidation of the hydroxyl groups of the dextran into aldehydes followed by reaction with amine functionalised NIR dye, iFluor 780 amine, and stabilisation by reductive amination using cyanogen bromide. This method resulted in only minor precipitation and the measured NIR signal was linear (Figure 14 left). Despite that, the conjugate did not appear to be stable *in vivo* as when evaluated in a small (2 mice/group) pilot experiment; no signal was detected above that of the untreated control. (Figure 14 right).
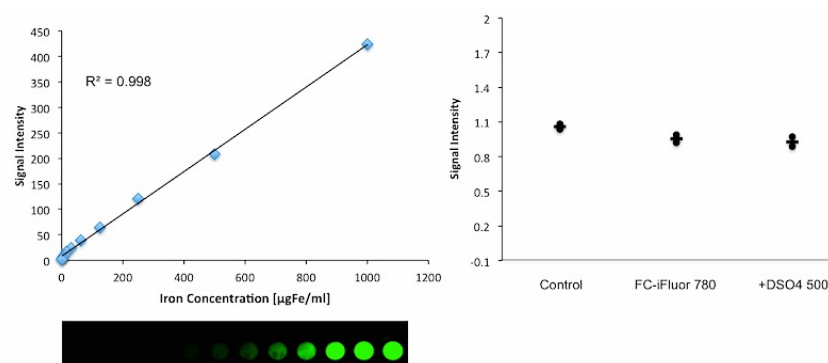
Figure 14: Results of conjugation of FC to iFluor 780 amine. **Left:** A linear increase (R^2=0.998) in the signal of the conjugate was seen as the iron concentration increased *in vitro,* images of individual wells illustrating florescence intensity are shown below. **Right:** Dot plot showing the mean signal intensity (bar) (n=2) for mice treated with FC-iFluor 780 with and without pre-treatment with DSO4 500. No signal above the control blood (untreated mice) was seen in all the treatment groups. Each mouse is represented by a circle (•).

The third method investigated for functionalising Ferucarbotran was to employ click chemistry attachment to carboxylic groups present in the carboxydextran coat. The method combines the use of EDC/NHS to conjugate Ferucarbotran to a DBCO-amine linker, which is subsequently "clicked" with an IRDye® 800CW azide dye. This reaction maintained the stability of the particles with no visible changes in the conjugate solution as well as only a slight increase in the hydrodynamic diameter after the conjugation. To confirm the success of labelling a serial dilution of the conjugate (FC-IRDye 800) was measured on Odyssey® scanner and a linear relationship was observed between the iron concentration and the signal intensity (Figure 15).
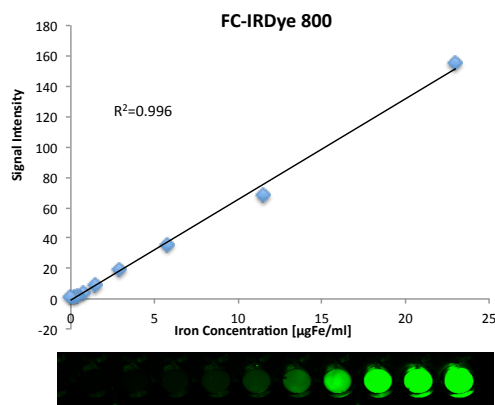

Figure 15: A linear relationship (R^2=0.99) was observed between the iron concentration of FC-IRDye 800 and the signal intensity as measured on Odyssey® scanner. Below: Images of individual wells illustrating florescence intensity are shown.

The conjugate was subsequently tested *in vivo*. Figure 16 shows a box plot of 4 different experiments performed with 4 different batches of FC-IRDye 800. In mice pre-treated with DSO4 500 24 hours prior to FC-IRDye 800 injection, a statistically significant (p=0.0039, Tukey HSD test) 5-fold increase in the blood signal was seen in the blocked group.

After confirming that prior blocking with DSO4 500 for 24 hours can increase the blood concentration of FC-IRDye 800, we also investigated this blocking effect at 3 different blocking times: either FC-IRDye 800 and DSO4 500 were given simultaneously (0 hours), or the blocker was given either 2 hours or 24 hours prior to FC-IRDye 800. Results in Figure 17 show that administration of DSO4 500 increased the blood concentration of FC-IRDye 800 at all the tested blocking times and the highest effect was seen at 24 hours.
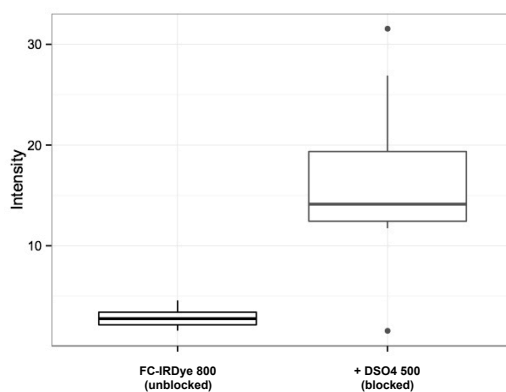

Figure 16: Box plot of FC-IRDye 800 treated mice with and without blocking showing a significant increase in the signal of FC-IRDye 800 in the blood of blocked mice compared to unblocked control (p=0.0039). Median signal intensity of blocked group is 14.13 compared to 2.76 in unblocked control.
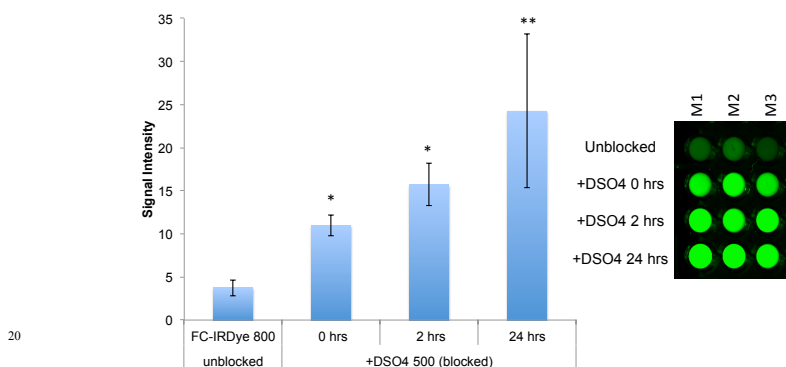

Figure 17: Signal of FC-IRDye 800 remaining in the blood of mice pre-treated with DSO4 500 with different blocking times. All blocking times tested have shown an improvement in the blood concentration of FC-IRDye 800 with the highest observed with 24 hour blocking. *p=0.001 **p=0.01 compared to unblocked control, bars represent mean values and error bars are for standard deviation. **Right:** Images of individual wells illustrating florescence intensity are shown. M1, M2 and M3 stand for mouse number.

Discussion

The rapid clearance of the SPIONs by the RES is advantageous when SPIONs are used as liver contrast agent (e.g. Resovist[®] and Endorem[®]) because it results in localisation of the particles within the Kupffer cells in healthy liver tissues, causing
5   a signal loss in MRI, compared to tumour cells that have lower phagocytic function[38]. This enables the differentiation of cancerous lesions from normal tissues and consequently their improved detection [38]. However if SPIONs are to be used in other clinical applications such as hyperthermia or as drug carriers, the rapid RES-mediated clearance becomes a problem.

10   A number of approaches have been taken to increase the circulating half-life of SPIONs by modifying their surface or using a smaller size. For example PEG coating of the particles has been used to prevent their adsorption and agglomeration [12, 39]. Others have used stealth surface modification with folic acid and o-carboxymethyl chitosans (OCMCS) to evade the RES as well as target the SPIONs
15   to tumours expressing folate receptor [40]. In this study, a 27 % reduction in the T2-weighted MRI signal intensity was observed in mice bearing folate receptor positive tumours and receiving the targeted/stealth SPIONs [40]. Decreasing the hydrodynamic diameter of the particles by using ultra small SPIONs (USPIO) (with diameters less than 50 nm) has also been shown to increase their half-life [20].

20   For our study, we took an alterative approach of blocking the RES, allowing use of clinically validated SPIONs such as Ferucarbotran. DSO4 500 was chosen as it is known to block liver Kupffer cells *in vivo* [41-49], and has been reported to block SPION uptake by macrophages *in vitro* [50, 51]. To prove the hypothesis that DSO4 500 can block liver uptake of SPIONs *in vivo*, SPIONs were labelled with NIR dye
25   to obtain a simple and quantitative means to measure their concentration in the blood.

Nanomag-D-spio amine is readily labelled with an NHS ester NIR dye and thus it was used to establish experimental conditions. Labelling Ferucarbotran was challenging because the functional groups available on the carboxydextran coating
30   do not allow a straightforward method of conjugation. Furthermore, the majority of commercially available NIR dyes are functionalised with either NHS ester or maleimide, to react with amines and sulfhydryl groups, respectively. These moieties are abundantly present in biomolecules but not on Ferucarbotran where the available chemical groups are either hydroxyl or carboxylic.

35   First we investigated labelling to hydroxyl groups using either epichlorohydrin or periodate oxidation but neither of these proved suitable for *in vivo* use. Epichlorohydrin chemistry resulted in particle aggregation and SPIONs labelled by periodate oxidation were not detectable *in vivo*. The latter might be related to physical changes leading to rapid clearance *in vivo*. Another explanation could be
40   the low labelling efficiency; however attempts to optimise labelling conditions resulted in SPIONs aggregation. This could have been aggravated by breaking the hexose rings of dextran during the reaction to form aldehydes.

Our most successful functionalisation of Ferucarbotran was achieved via the carboxylic groups using a combination of the standard EDC/NHS reaction to a
45   dibenzocyclooctyne-amine linker followed by a copper free click reaction with the azide dye. This reaction is performed in mild conditions, which helps to maintain the stability of the particles.

The effect of conjugation on the superparamagnetic properties of SPIONs was evaluated to ensure that they were not affected during the conjugation process. No major differences were observed in the hysteresis loops of SPIONs as measured on SQUID. In addition, successfully conjugated SPIONs (NM-DyLight 800 and FC-IRDye 800) showed no significant changes in the hydrodynamic diameter or PDI compared to unmodified SPIONs.

In vivo, pre-treatment with DSO4 500 showed a median 15-fold improvement in the signal intensity of NM-DyLight 800, compared to a median 5-fold improvement with FC-IRDye 800. Thus, in our pilot experimental conditions, DSO4 500 appeared to be more effective in reducing the clearance of Nanomag-D-spio-NH_2 than of Ferucarbotran (Figure 12 and 16). Consequently, our future work with NIR functionalised SPIONs will focus on optimising the experimental conditions required to maximise the pharmacokinetic profiles for individual nanoparticles.

The work presented in this paper provides methods to functionalise SPIONs with dyes that allow sensitive measurements of their blood concentrations. The labelled SPIONs have been used *in vivo* to demonstrate that RES blockers, such as DSO4 500, can prolong SPIONs half-life potentially widening their clinical applications.

References

1. K. M. Krishnan, *IEEE Transactions on Magnetics*, 2010, **46**, 2523-2558.
2. A. K. Gupta, R. R. Naregalkar, V. D. Vaidya and M. Gupta, *Nanomedicine*, 2007, **2**, 23-39.
3. B. Hamm, T. Staks, M. Taupitz, R. Maibauer, A. Speidel, A. Huppertz, T. Frenzel, R. Lawaczeck, K. J. Wolf and L. Lange, *Journal of Magnetic Resonance Imaging*, 1994, **4**, 659-668.
4. R. Lawaczeck, H. Bauer, T. Frenzel, M. Hasegawa, Y. Ito, K. Kito, N. Miwa, H. Tsutsui, H. Vogler and H. J. Weinmann, *Acta Radiologica*, 1997, **38**, 584.
5. B. Bonnemain, *J Drug Target*, 1998, **6**, 167-174.
6. P. Reimer and T. Balzer, *European radiology*, 2003, **13**, 1266-1276.
7. C. Sun, J. S. H. Lee and M. Zhang, *Advanced drug delivery reviews*, 2008, **60**, 1252-1265.
8. M. Plotkin, U. Gneveckow, K. Meier-Hauff, H. Amthauer, A. Feußner, T. Denecke, M. Gutberlet, A. Jordan, R. Felix and P. Wust, *International journal of hyperthermia*, 2006, **22**, 319-325.
9. G. L. DeNardo and S. J. DeNardo, *Cancer biotherapy & radiopharmaceuticals*, 2008, **23**, 671-680.
10. K. Maier-Hauff, F. Ulrich, D. Nestler, H. Niehoff, B. Thiesen, H. Orawa, V. Budach and A. Jordan, *Journal of neuro-oncology*, 2011, 1-8.
11. C. Vauthier, N. Tsapis and P. Couvreur, *Nanomedicine*, 2011, **6**, 99-109.
12. A. K. Gupta and M. Gupta, *Biomaterials*, 2005, **26**, 3995-4021.
13. J. Dobson, *Drug development research*, 2006, **67**, 55-60.
14. W. H. De Jong and P. J. A. Borm, *International journal of nanomedicine*, 2008, **3**, 133.

15.   B. H. Park, J. C. Jung, G. H. Lee, T. J. Kim, Y. J. Lee, J. Y. Kim, Y. W. Kim, J. H. Jeong and Y. Chang, *Colloids and Surfaces A: Physicochemical and Engineering Aspects*, 2008, **313**, 145-149.
16.   V. Mailänder, M. R. Lorenz, V. Holzapfel, A. Musyanovych, K. Fuchs, M. Wiesneth, P. Walther, K. Landfester and H. Schrezenmeier, *Molecular Imaging and Biology*, 2008, **10**, 138-146.
17.   M. R. Loebinger, P. G. Kyrtatos, M. Turmaine, A. N. Price, Q. Pankhurst, M. F. Lythgoe and S. M. Janes, *Cancer research*, 2009, **69**, 8862.
18.   A. Chachuat and B. Bonnemain, *Der Radiologe*, 1995, **35**, S274.
19.   D. Simberg, J.-H. Park, P. P. Karmali, W.-M. Zhang, S. Merkulov, K. McCrae, S. N. Bhatia, M. Sailor and E. Ruoslahti, *Biomaterials*, 2009, **30**, 3926-3933.
20.   C. Chouly, D. Pouliquen, I. Lucet, J. Jeune and P. Jallet, *Journal of microencapsulation*, 1996, **13**, 245-255.
21.   S. Majumdar, S. Zoghbi and J. Gore, *Investigative radiology*, 1990, **25**, 771-777.
22.   L. Maurizi, U. Sakulkhu, A. Gramoun, J.-P. Vallee and H. Hofmann, *Analyst*, 2014.
23.   V. R. Kondepati, H. M. Heise and J. Backhaus, *Analytical and bioanalytical chemistry*, 2008, **390**, 125-139.
24.   J. G. Kim, M. Xia and H. Liu, *Engineering in Medicine and Biology Magazine, IEEE*, 2005, **24**, 118-121.
25.   Micromod-Partikeltechnologie-GmbH, *Nanomag-D-spio Technical Data Sheet*, 2012.
26.   D. T. Kehagias, A. D. Gouliamos, V. Smyrniotis and L. J. Vlahos, *Journal of Magnetic Resonance Imaging*, 2001, **14**, 595-601.
27.   P. Reimer, E. J. Rummeny, H. E. Daldrup, T. Balzer, B. Tombach, T. Berns and P. E. Peters, *Radiology*, 1995, **195**, 489-496.
28.   K. Shamsi, T. Balzer, S. Saini, P. R. Ros, R. C. Nelson, E. C. Carter, S. Tollerfield and H. P. Niendorf, *Radiology*, 1998, **206**, 365-371.
29.   C. E. Balzer T, Shamsi K, Niendorf HP, *Academic radiology*, 1996, **3 suppl 2:1996 Aug pg S417-9**.
30.   T. Hao-Yu, L. Chen-Yi, S. Ying-Hsia, L. Xi-Zhang and L. Gwo-Bin, Nano/Micro Engineered and Molecular Systems, 2007. NEMS '07. 2nd IEEE International Conference on, 2007.
31.   H. Y. Tseng, G. B. Lee, C. Y. Lee, Y. H. Shin and X. Z. Lin, *Nanobiotechnology, IET*, 2009, **3**, 46-54.
32.   S. Takamatsu, O. Matsui, T. Gabata, S. Kobayashi, M. Okuda, T. Ougi, Y. Ikehata, I. Nagano and H. Nagae, *Radiation Medicine*, 2008, **26**, 179-187.
33.   T. Araya, K. Kasahara, S. Nishikawa, H. Kimura, T. Sone, H. Nagae, Y. Ikehata, I. Nagano and M. Fujimura, *OncoTargets and therapy*, 2013, **6**, 237.
34.   K. Yamada, T. Oda, S. Hashimoto, T. Enomoto, N. Ohkohchi, H. Ikeda, H. Yanagihara, M. Kishimoto, E. Kita and A. Tasaki, *International Journal of Hyperthermia*, 2010, **26**, 465-474.
35.   M. J. Pittet, F. K. Swirski, F. Reynolds, L. Josephson and R. Weissleder, *Nature protocols*, 2006, **1**, 73-79.
36.   D. J. Maxwell, J. Bonde, D. A. Hess, S. A. Hohm, R. Lahey, P. Zhou, M. H. Creer, D. Piwnica-Worms and J. A. Nolta, *Stem Cells*, 2007, **26**, 517-524.
37.   K. L. Vigor, P. G. Kyrtatos, S. Minogue, K. T. Al-Jamal, H. Kogelberg, B. Tolner, K. Kostarelos, R. H. Begent, Q. A. Pankhurst and M. F. Lythgoe, *Biomaterials*, 2010, **31**, 1307-1315.
38.   G. M. Lanza, P. M. Winter, S. D. Caruthers, A. M. Morawski, A. H. Schmieder, K. C. Crowder and S. A. Wickline, *Journal of nuclear cardiology*, 2004, **11**, 733-743.
39.   V. P. Torchilin and V. S. Trubetskoy, *Advanced drug delivery reviews*, 1995, **16**, 141-155.
40.   C. Fan, W. Gao, Z. Chen, H. Fan, M. Li, F. Deng and Z. Chen, *International journal of pharmaceutics*, 2011, **404**, 180-190.
41.   J. W. Bradfield, R. L. Souhami and I. E. Addison, *Immunology*, 1974, **26**, 383-392.
42.   K. R. Patel, M. P. Li and J. D. Baldeschwieler, *Proceedings of the National Academy of Sciences*, 1983, **80**, 6518.
43.   L. Illum, N. W. Thomas and S. S. Davis, *Journal of pharmaceutical sciences*, 1986, **75**, 16-22.
44.   N. Das, M. K. Basu and M. K. Das, *Bioscience Reports*, 1987, **7**, 465-470.
45.   H. Sands and P. L. Jones, *Journal of nuclear medicine: official publication, Society of Nuclear Medicine*, 1987, **28**, 390.

46. R. W. Jansen, G. Molema, T. L. Ching, R. Oosting, G. Harms, F. Moolenaar, M. J. Hardonk and D. K. Meijer, *Journal of Biological Chemistry*, 1991, **266**, 3343.
47. D. Liu, A. Mori and L. Huang, *Biochimica et Biophysica Acta (BBA)-Biomembranes*, 1992, **1104**, 95-101.
48. T. Yoshinobu, F. Takuya, F. Hisao, N. Makiya, S. Hitoshi and H. Mitsuru, *International journal of pharmaceutics*, 1994, **105**, 19-29.
49. M. Fujiwara, J. D. Baldeschwieler and R. H. Grubbs, *Biochimica et Biophysica Acta (BBA)-Biomembranes*, 1996, **1278**, 59-67.
50. O. Lunov, V. Zablotskii, T. Syrovets, C. Röcker, K. Tron, G. U. Nienhaus and T. Simmet, *Biomaterials*, 2010.
51. C. Y. Yang, M. F. Tai, C. P. Lin, C. W. Lu, J. L. Wang, J. K. Hsiao and H. M. Liu, *PloS one*, 2011, **6**, e25524.